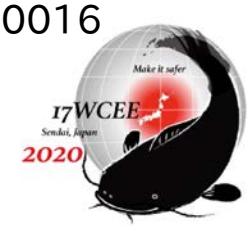

OBSERVED DAMAGE AT SCHOOLS AFTER THE ILLAPEL EARTHQUAKE (CHILE, 2015)

F. López-Almansa[(1)], G. Valdebenito[(2)], S. Bustos[(3)]

[(1)] *Professor, Technical University of Catalonia, Architecture Technology Department, Barcelona, francesc.lopez-almansa@upc.edu; currently Associate Researcher Faculty of Engineering, Natural and Anthropogenic Risks Research Center, Univ. Austral de Chile, Valdivia*

[(2)] *Professor, Natural and Anthropogenic Risks Research Center, Univ. Austral de Chile, Valdivia, gvaldebenito@uach.cl*

[(3)] *Associate Researcher, Natural and Anthropogenic Risks Research Center, Univ. Austral de Chile, Valdivia, simon.bustos@uach.cl*

Abstract

At 7:54 pm September 16th 2015, a M_w = 8.4 earthquake shook the Coquimbo region, northern-central Chile. The epicentral coordinates are 71.741º W and 31.637º S (46 km offshore); the hypocentral depth is 23 km, hence, this event is considered as an interplate earthquake (subduction of the Nazca plate under the South American plate). The rupture length is in between 200 and 250 km, and the maximum displacement ranges between 5 and 6 m. In the involved segment of the trench, the fault plane is located between 90 and 150 km offshore, with 50 km depth; the subduction angle is approximately 19º. A number of aftershocks followed the main shake; the strongest one reached M_w = 7.6 (8:18 pm September 16th 2015). The Illapel earthquake was recorded at fifteen stations; the maximum recorded acceleration is 0.81 g, EW component in Monte Patria Station. Important tsunamis were generated; the tallest wave reached 4.5 m. This event (commonly known as Illapel earthquake) killed 15 people and injured severely 5, destroyed 2442 homes and damaged seriously 2712, and left homeless 27722 people; the intensity in the IMM scale is VIII ("severe damage").

Most of the damage caused by the Illapel earthquake concentrated in poorly designed school and hospital buildings; this paper presents a study of the observed damage in the school buildings. Four representative schools are particularly discussed: "El Ingenio" school in Ovalle, children school in Coquimbo, "Maritima" school in Tongoy, and, mainly, "San Rafael de Rozas" school in Illapel. Their damage is comprehensively described; it is understood in terms of poor design, site effects and other relevant issues. Regarding the seismic design, the role of short columns is thoroughly investigated, among other structural deficiencies. Concerning the site effects, the soil fundamental period is identified after by two types of ambient vibration field tests: Nakamura, and soil profile analysis by using geophones. The natural periods of the damaged buildings were identified after operational modal analysis using triaxial seismometers. Then, the proximity between and the soil and the structure fundamental period is investigated as a main potential source of response amplification.

Further research includes a detailed study on a particular case (San Rafael de Rozas school, Illapel); this study incorporates numerical simulation of the dynamic soil and building response.

Keywords: Chile; Illapel Earthquake; School Buildings; Operational Modal Analysis; Observed Damage.

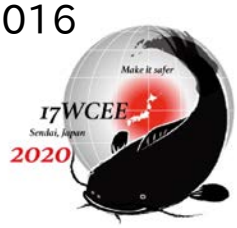

1. Illapel earthquake

Most of the Chilean seismicity is generated by the subduction of the Nazca plate under the South American one; given that their relative velocity is rather high (approximately 9-10 cm/year) and that the subduction interface is commonly blocked, there are strong stress accumulations, with frequent violent releases, thus generating severe ground shakings and tsunamis. These seismic events can be broadly classified into three categories: interplate (the hypocentral depth ranges between 0 and 60 km), intraplate (the hypocentral depth ranges between 60 and 200 km) and cortical. The cortical earthquakes are caused by the deformation of the continental plate, thus being rather shallow; their hypocentral depth does not exceed commonly 40 km. Finally, some outer-rise (off-shore) events have been reported, being extremely shallow, with hypocentral depth ranging between 0 and 15 km.

In the Coquimbo region, 577 earthquakes with $M_w \geq 5.5$ have been reported since 1900 [1], this bustle representing 49% of the total seismic activity in Chile. Among these ground motions, 412 are interplate, 99 intraplate, 58 cortical and 8 outer-rise. Five of these events had $M_w \geq 7$: 17 August 1906 (M_w = 8.2), 6 April 1943 (M_w = 8.1), 19 April 1955 (M_w = 7.0), 14 October 1997 (M_w = 7.1) and, finally, the Illapel earthquake 16 September 2015 (M_w = 8.4) [1]. Figure 1.a depicts the locations of the epicenters of such events, and Figure 1.b refers specifically to the Illapel one.

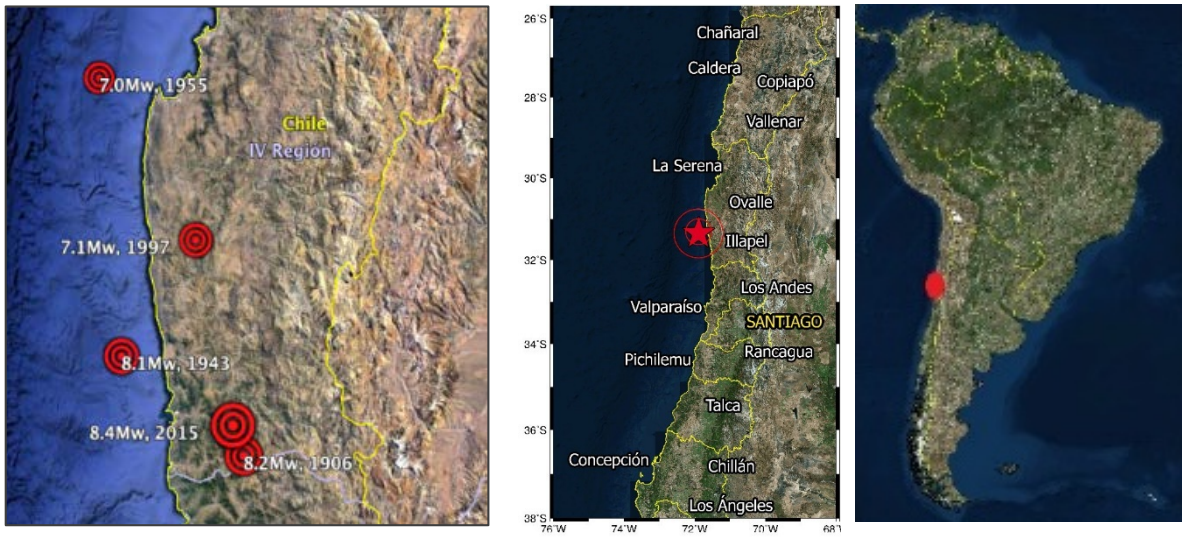

(a) Seismic events with $M_w \geq 7$ [1] (b) Illapel earthquake [2]

Figure 1. Seismicity in the Coquimbo region

The 1955 earthquake is outer-rise, the 1943 and 1997 ones are considered as intraplate, and the 1906 and 2015 ones are interplate. Noticeably, these last two events correspond to similar and closely located ruptures. Figure 1 shows that the Illapel earthquake is the most severe ever registered in the Coquimbo region. The focal mechanism was mainly vertical, thus causing greater structural damage, due to the high amplitude of the S waves.

The main shake of the Illapel earthquake occurred in September 16th 2015 at 7:54 pm. The epicentral coordinates are 71.741º W and 31.637º S (46 km offshore); the hypocentral depth is 23 km, hence, this event is considered as an interplate earthquake. The rupture length is in between 200 and 250 km, and the maximum displacement ranges between 5 and 6 m. In the involved segment of the trench, the fault plane is located between 90 and 150 km offshore, with 50 km depth; the subduction angle is approximately 19º. A number of aftershocks followed the main shake; the strongest one reached M_w = 7.6 (16 September 2015 8:18 pm) and over 140 aftershocks with M_w > 5.0 have been reported so far. The hypocentral depth of most of the aftershocks is less than 60 km; therefore, such events are classified as interplate. Important tsunamis were generated; the

tallest wave reached 4.5 m. Damage was significant: 15 people died and 5 were severely injured, 2442 homes were destroyed and 2712 seriously damaged, and 27722 persons were left homeless.

The Illapel earthquake was recorded at fifteen seismological stations. Figure 2.a displays the locations of such stations (each location is accompanied by a plot of the recorded E-W component), and Figure 2.b depicts the distribution of Intensities in the Mercalli scale. Table 1 displays the maximum recorded accelerations at each station.

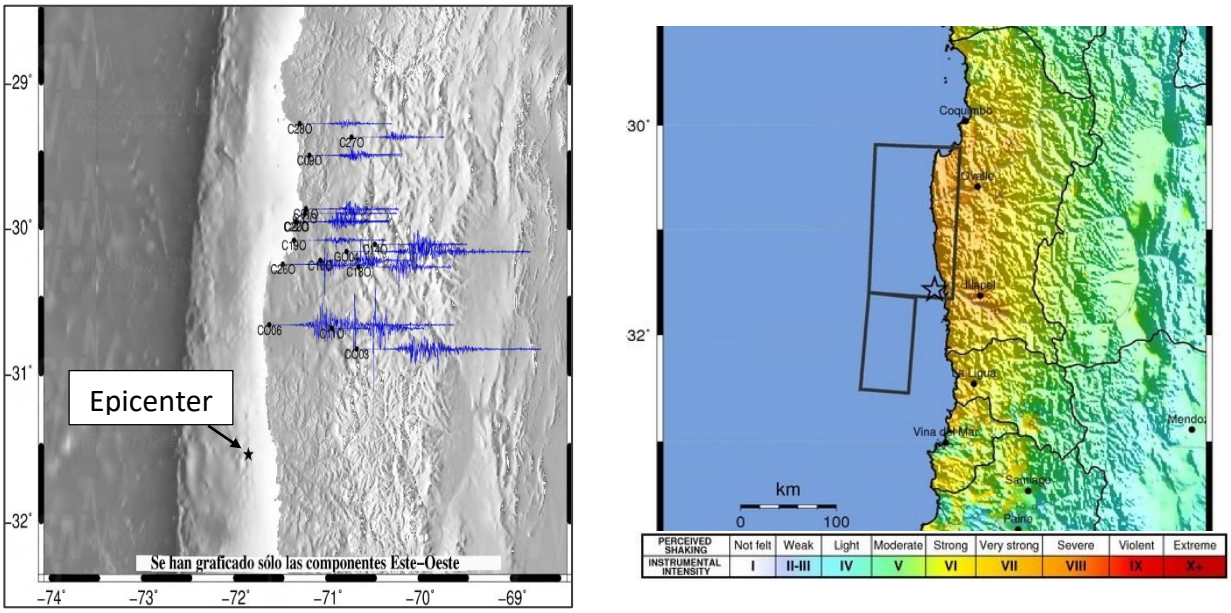

(a) Map of seismological stations [3] (b) Intensities in the Mercalli scale [1]

Figure 2. Effects of the Illapel earthquake

Table 1 – Maximum recorded accelerations in the Illapel earthquake [3]

Station	Locality	Coordinates (°)		PGA (g)		
		Latitude (S)	Longitude (W)	EW	NS	Z
C110	Monte Patria	30.46	71.33	0.814	0.699	0.466
C180	Paiguano	30.04	70.32	0.471	0.496	0.228
C260	Tongoy	29.384	70.745	0.357	0.230	0.131
C003	Pedregal	30.09	70.56	0.341	0.283	0.197
C006	Angostura	30.123	70.491	0.336	0.354	0.193
C100	Vicuña	29.877	71.238	0.306	0.289	0.183
C140	Vicuña	30.278	70.669	0.292	0.172	0.161
C200	Coquimbo	29.59	71.19	0.251	0.249	0.178
G004	Cerro Tololo	29.47	71.19	0.233	0.337	0.155
C090	La Higuera	30.04	71.21	0.183	0.184	0.092
C010	Las Compañías	29.291	71.308	0.151	0.173	0.118
C330	La Serena	30.5	70.55	0.137	0.108	0.068
C270	Los Cuartitos	30.13	71.27	0.124	0.092	0.051

Table 1 shows that the maximum recorded acceleration is 0.81 g, corresponding to the Monte Patria Station, EW component. Comparison between Figure 2 and Table 1 shows that the accelerations attenuate with the distance to the epicenter. The mostly affected localities are Illapel, Ovalle and Salamanca; the intensity in the IMM scale is VIII (“severe damage”). As discussed more deeply in section 2, most of the damage concentrated in poorly designed school and hospital buildings.

2. Field study of the damaged school buildings

2.1. Campaign description

After the main seismic event, a 5-day (October 5-9 2015) field inspection was undertaken in the Coquimbo Region. The campaign was lead by RiNA (Natural and Anthropogenic Risks Research Center) of the Universidad Austral de Chile. The main objectives were:

- Observation and evaluation of damaged structures, mainly school buildings.
- Geophysical surveys based on the HSVR technique (Nakamura method) [4] and Constrained H/V + ReMi passive seismic arrays (Refraction Microtremor) [5-6] in order to obtain some basic soil dynamic parameters and to evaluate the site-effects, trying to correlate them with the observed damage.
- Operational Modal Analysis (OMA) [7] of the damaged buildings (wherever possible) in order to obtain some basic information of their current dynamic properties.
- Calibration of the new tool TiDHA® [8]. This is a software developed at RiNA for fast field after-earthquake evaluation of damaged buildings.

Four school buildings were visited; next three subsections describe the first three cases, and the fourth case is discussed more deeply in section 3 and in the rest of the paper.

2.2. “El Ingenio” school in Ovalle

This building was only moderately damaged. The school has two stories and the structure is made of concrete, consisting in a combination of shear walls and moment-resisting frames. The earthquake caused a slight settlement in the west wing; non-structural damage of the ceilings was also observed. Figure 3.a presents a general view of such west wing, and Figure 3.a depicts the aforementioned damage of the ceilings.

(a) General view of the west wing

(b) Nonstructural damage of the ceilings

Figure 3. “El Ingenio” School, Ovalle

Apparently, plan symmetry and regularity in elevation plaid a relevant role in the rather good seismic performance of this building.

2.3. Children school in Coquimbo

Although very slight damage was observed in this 2-story building, it is interesting to expose a typical masonry Chilean school building being located in an area where the Illapel earthquake notably affected masonry housing buildings. Figure 4.a shows the damage on a wall originated by bending rotation of the beam-wall connection; as well, probably, the slab experienced also some pounding. Additionally, Figure 4.b describes part of the performed geophysical surveys.

(a) Cracking originated by rotation of the wall-beam connection

(b) ReMi seismic survey

Figure 4. Children School, Coquimbo

2.4. "Marítima" school in Tongoy

Figure 5 shows that this school is a complex of 2 and 3-story buildings; it is located at the sea side.

Figure 5. General view of the complex Marítima School, Tongoy

The complex consists of several connected masonry and RC frame buildings. The observed damage was only slight; Figure 6.a presents some damage in column-beam joints and Figure 6.b describes the damage of a connecting bridge. Apparently, this last damage was caused by incorrect design of the bridge supports.

(a) Slight damage in some connections

(b) Damage in the bridge connection

Figure 6. Observed damage at the Marítima School

3. San Rafael de Rozas school building

3.1. Building description

This building was the most damaged among the visited ones. For that reason, it is more deeply analyzed in this section and in the next ones.

The school building is located in downtown Illapel, belonging to the Coquimbo region (283 km North to Santiago); it had been designed and built in 2003. Three wings compose the building; are separated by seismic joints. The central wing has three stories and L-shaped plan layout, and the external wings are rectangular, being attached to both ends of the central one. Figure 7 describes the global characteristics of the building.

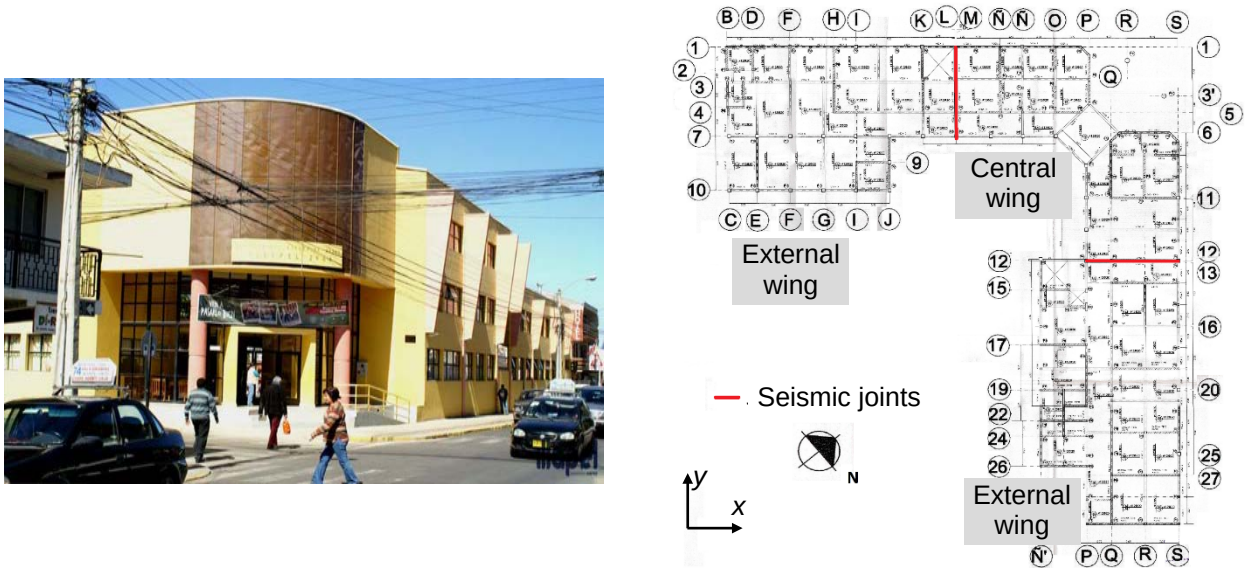

(a) General view (b) Plan layout

Figure 7. San Rafael de Rozas school building

Figure 7.a displays the main building entrance, being located in the corner of the central wing. Figure 7.b represents the first floor plan layout. This paper focusses in the central wing, having been the most damaged part during the quake.

The plan size of the analyzed central wing is 23.9 m and 24.1 m in *x* and *y* directions, respectively (Figure 7.b); their height is 10.31 m. Noticeably, such axes (*x*, *y*, *z*) are maintained along the rest of the paper. The structure consists of 3-D RC moment-resisting frames (columns and slabs with beams joining the columns in both directions) and unreinforced or confined masonry infill walls [9]. Noticeably, some of the walls do not cover the full column height, thus generating relevant dangerous short column effects; in these cases, such walls are topped with tying beams (known as “cadenas” –chains– in Chile) that are properly anchored to the columns.

Figure 8 displays detailed plan views of the analyzed central wing structure; Figure 8.a, Figure 8.b, Figure 8.c and Figure 8.d correspond to the foundation and the first, second and third stories, respectively. For further clarity, the full and incomplete walls are represented in Figure 8 with dark blue and light blue segments, respectively.

(a) Foundation (b) First story

(c) Second story (d) Third story

Figure 8. Structural plan layout of the central wing

Figure 8 shows that the slabs are composed of beams (their sections range between 20 cm × 40 cm and 20 cm × 60 cm) and 15 cm deep solid slabs. The rectangular columns range between 15 cm × 20 cm and 35 cm × 35 cm, and the circular columns in the main entrance (Figure 7.a) have 60 cm diameter. The thickness of the masonry infill walls is 20 cm. The foundation beams (Figure 8.a) are 15 cm × 30 cm. The transverse reinforcement consists in hoops made of 6 mm bars at each 17-20 cm and 8 mm bars separated 17 cm.

The seismic weight of the wing is 7959 kN. According to the Chilean design code [10] this weight should correspond to $D + 0.25\,L$, where D and L refer to dead and live load, respectively; however, given that the earthquake occurred at 7.54 pm (Section 1), it is assumed that the school was empty at that time, and the contribution of the live load has been disregarded.

3.2. Observed damage

Two types of damage were observed: brittle shear failure of short columns, and extended cracking of confined masonry walls. Figure 9 displays representative examples of such failure types.

(a) Highly damaged short column

(b) Damaged short column

(c) Cracked infill wall

Figure 9. Observed damage in the analyzed wing

Figure 9.a represents the failure of a short column that is adjacent to a column belonging to an external wing (Figure 7.b); this explains the apparent asymmetry of the damage, as left (counterclockwise) shear strain was prevented by such column. Figure 9.b depicts the shear failure of a short column. Noticeably, the transverse reinforcement (6 mm diameter hoops separated 17 cm) proved totally insufficient. Figure 9.c illustrates the crushing of the top corner of an infill wall; this type of failure corresponds to the classical diagonal compression strut mechanism [11].

3.3. Soil characterization

The foundation soil is characterized by two types of ambient vibration field tests: Nakamura [4], and soil profile analysis by using geophones. Both studies are described next.

Nakamura. Two ambient vibration measurements using the Micromed TROMINO seismograph were carried out in the points marked as 1 and 2 in Figure 10.a.

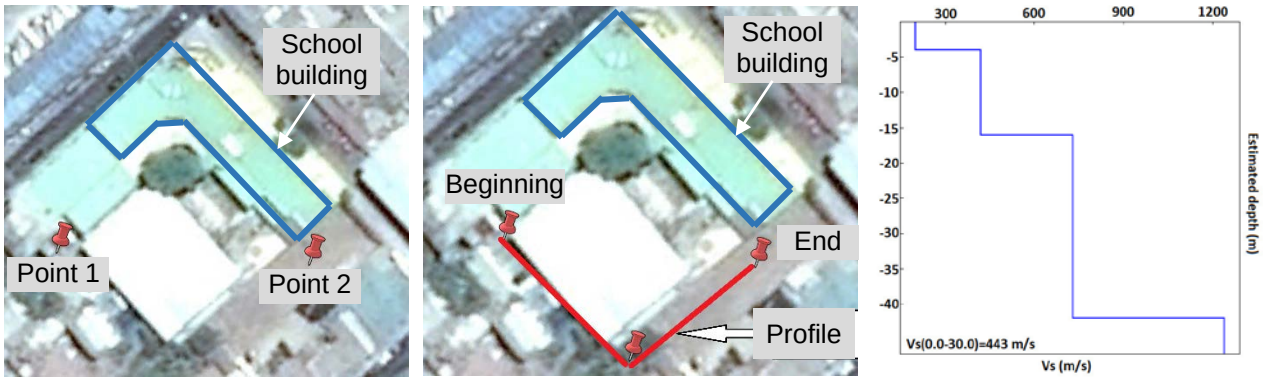

(a) Points for Nakamura tests

(b) Analyzed L-shaped soil profile

(c) Vertical soil profile

Figure 10. Soil field tests in the San Rafael de Rozas School, Illapel

Each measurement lasted 16 minutes; the sampling rate was 128 Hz. Vertical and horizontal (NS and EW) velocities were recorded. These signals were processed as indicated in [12]. Figure 11 displays the Fourier

spectra of the ratio between the vertical and the horizontal components; Figure 11.a and Figure 11.b correspond to points 1 and 2, respectively.

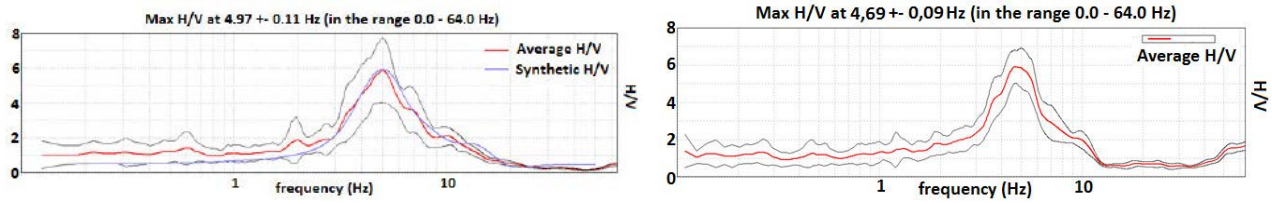

(a) Point 1 (b) Point 2

Figure 11. H / V spectra in Illapel

Figure 11 shows a peak for a frequency approximately equal to 5 Hz; hence, the soil fundamental period should be near to 0.2 s. Comparison between the spectra in Figure 11.a and Figure 11.b shows high similarity; therefore, the soil appears to be rather uniform.

Soil profiles. Micro seismic superficial refraction passive techniques Constrained H/V [5] and Refraction Microtremor (ReMi) [6] have been utilized. These techniques are mainly based in measuring the Rayleigh wave velocity; both are combined to take better advantages and compensate their limitations [13]. The analyzed L-shaped soil profile is described in Figure 10.b; each side measured 35 m. Velocity sensors (geophones) were installed every 5 m; their eigenfrequency was 4.5 Hz. Figure 10 displays the obtained soil profile.

Figure 10.c represents the shear wave velocity vs. soil depth. The harmonic weighted average for the top 30 m is $v_{s,30}$ = 443 m/s. According to the Chilean regulation [14] the soil type is C; however, given the absence of more conclusive information (such as boreholes), the soil is conservatively classified as D. This type corresponds to soil B according the European regulations [15] and soil C according the American specifications [16]. In any case, broadly speaking, the soil is rather stiff; moreover, Figure 10.c shows that, below 16 m, the soil is almost rock. These circumstances seem to indicate that no relevant site effects (seismic waves amplification) are expected.

3.4. Operational Modal Analysis

The objective of this study was to estimate the building major modal parameters (mainly, the natural periods in the main directions) after ambient vibration measurements. The analysis was conducted using a triaxial velocity and acceleration-sensitive seismograph; that device was installed near the center of mass, and was oriented according to the *x* and *y* axes (Figure 7.b). The sampling frequency was 512 Hz, and each measurement lasted approximately 6 minutes. Figure 12 displays the obtained spectra in E-W direction (Figure 12.a) and N-S (Figure 12.b) directions; the vertical components are not plotted, as being considered of little interest only.

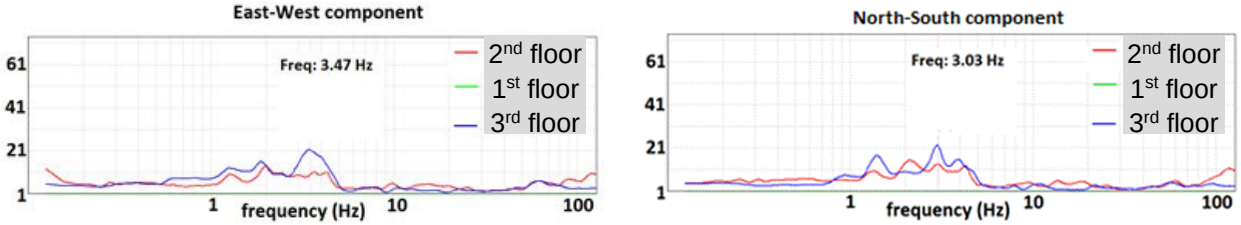

(a) E-W direction (b) N-S direction

Figure 12. Spectra in Illapel obtained after Operational Modal Analysis

Figure 12 shows that the spectra in both directions exhibit a peak near 0.3 s (0.288 s in Figure 12.a and 0.330 s in Figure 12.b); thus, the periods of the first translational modes in *x* and *y* directions should be close to that

value. Noticeably, given that only one accelerometer was installed at a given story, the torsional modes cannot be easily detected.

4. Numerical modelling of the San Rafael de Rozas school structural behavior

The nonlinear static and dynamic building structural behavior is described with a 3-D model implemented in the SAP2000 software code v. 20.2.0 [17]. The representation of each structural element in that model is described next.

- **Columns and beams**. Such members are modelled with 2-node 3-D frame elements; at each node, there are six degrees of freedom. Each column or beam is discretized into a single element. To account for the influence of concrete cracking, the initial bending and shear stiffness is reduced as indicated in the American specifications [16]. The nonlinear behavior of the short columns is described by shear plastic hinges located at their mid-section (Figure 9).
- **Walls**. The walls are described with strut-and-tie models; the ties are the involved segments of columns and the horizontal topping beams ("cadenas"), and the struts are diagonal compression-only members. Both struts and ties are pin-ended elements. The strut width is selected as one fourth of its length [11]. As no compression damage was observed in the walls, the strut behavior is modelled as linear; their stiffness is not of crucial importance, given that the strut-and-tie models can reproduce only the ultimate wall structural capacity, but not its initial stiffness, given the influence of their non-represented parts. Thus, the walls are discretized also with 4-node quadrilateral shell elements to be able to estimate the wall stiffness. This last model is only employed to identify the building parameters in the conducted operational modal analyses; therefore, its behavior is assumed to be linear.
- **Slabs**. The slabs are discretized with 4-node quadrilateral shell elements; at each node, there are six degrees of freedom. As in the columns and beams, the initial stiffness is reduced as specified in the American documents [16] (to account for the influence of tensioned concrete cracking). The slab is discretized into square elements (near 0.5 m × 0.5 m). Given the absence of observed damage in the slabs, their behavior is modelled as linear.
- **Foundation**. As shown by Figure 8.a, the building foundation consists of spread footings joined by foundation beams in a single direction. Such elements are modelled as constant-width beam (with average width).
- **Soil**. The soil flexibility is incorporated into the model; in other words, the SSI (Soil-Structure Interaction) is accounted for, although in a rather simplified way. Such flexibility is described with a vertical coefficient of ballast; it is estimated after the percentage of the CBR (California Bearing Ratio) penetration test. Given that, in the top 4 m, the shear wave velocity is less than 100 m/s (Figure 10), such percentage is taken as 9% [18]. Then, the coefficient of ballast (modulus of subgrade reaction) is obtained as $C_v = 0.25 + 5.15 \log_{10} 9 = 5.164$ kg/cm^3 [18]. Since the soil quality is regular, the horizontal coefficient is taken as 8% of the vertical one: $C_h = 0.08\ C_v = 0.413$ kg/cm^3 [19]. In the ensuing concentrated vertical and horizontal springs, the stiffness coefficients are obtained by multiplying the coefficient of ballast by the contributive area of the foundation (as described in the previous paragraph). For the spread footings, $k_v = C_v \times 120 \times 120 = 74{,}362$ kg/cm. Regarding the strip footings, the coefficient of ballast is corrected according to the strip aspect ratio, thus providing $C_v = 4.358$ kg/cm^3 [19]; then $k_v = C_v \times 100 \times 47 = 20{,}483$ kg/cm.

The mechanical parameters of the structural materials are described next. Regarding concrete, the characteristic value of the compressive strength is $f_c' = 250$ kg/cm^2, and the deformation modulus is $E_c = 15100 (f_c')^{½} = 238752$ kg/cm^2 [20]. About the reinforcement steel, the yield point is $f_y = 2{,}800$ kg/cm^2, the ultimate stress is $f_u = 4{,}400$ kg/cm^2, and the modulus of elasticity is $E_s = 2{,}100{,}000$ kg/cm^2 [21]. For the masonry, the unit weight is $\gamma_m = 1{,}800$ kg/m^3 [22], the characteristic value of the compressive strength is $f_m' = 40$ kg/cm^2 [9], and the deformation modulus is $E_m = 16{,}000$ kg/cm^2 (masonry); this last value has been obtained after the European regulations [23], as the provided values are considered to be more realistic.

Figure 13 displays a general view of the building central wing structural model. This sketch describes the discretization of the walls with strut-and-tie models; given that this model is initially intended for pushover (monotonic) analysis, only a single strut per wall is utilized.

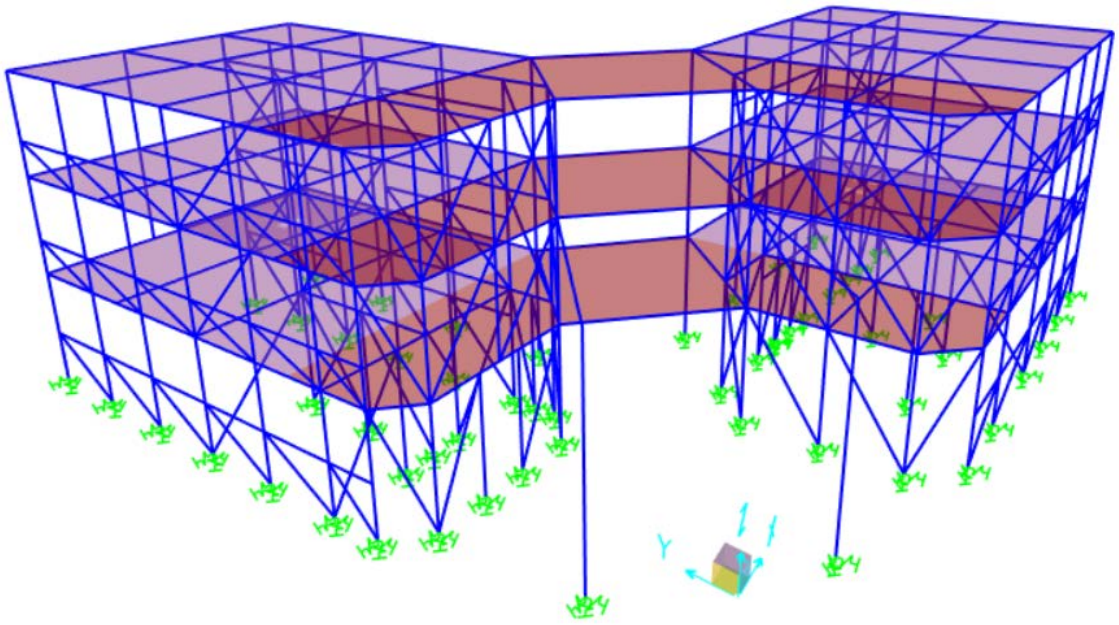

Figure 13. Structural model of the San Rafael de Rozas building central wing

5. Calibration of the San Rafael de Rozas school model with results from Operational Modal Analysis

The model described in section 5 is utilized is utilized to perform a modal analysis whose results can be compared with the experimental ones (subsection 3.4); this comparison allows to calibrate the aforementioned model.

The analyses are conducted in two different conditions, by considering the full section stiffness (i.e. based on the gross sectional parameters), and by considering the stiffness decrease due to concrete cracking; this last operation is performed with the reduction coefficients in [16]. In the first case, the first three natural periods are: $T_1 = T_\varphi = 0.365$ s (torsion), $T_2 = T_x = 0.316$ s (x direction), and $T_3 = T_y = 0.287$ s (y direction); in the second case, the periods are: $T_\varphi = 0.39$ s, $T_x = 0.33$ s, and $T_y = 0.30$ s. Comparison among both sets of results shows that the influence of concrete cracking is only moderate.

Comparison between these numerical results and the experimental ones in subsection 3.4 shows a rather reasonable agreement, given the higher uncertainty of both numerical and experimental studies.

6. Conclusions

This paper discusses observed damage of school buildings in central Chile caused by the $M_w = 8.4$ Illapel earthquake (16/09/2015). Preliminary results seem to indicate that the buildings were damaged mainly because of conceptual design errors. In this sense, the most affected school (San Rafael de Rozas, Illapel) had many short columns, being responsible for most of the destruction. This conclusion is corroborated by numerical simulation; the employed model is calibrated with Geophysical Surveys and Operational Modal Analyses.

7. Acknowledgements

This work has received financial support from Spanish Government under projects BIA2014-60093-R and CGL2015-6591 (Feder funds). These supports are gratefully acknowledged.

8. References

[1] USGS (2020). Science for a changing world. Available at https://earthquake.usgs.gov/earthquakes/. Last access: 2020.

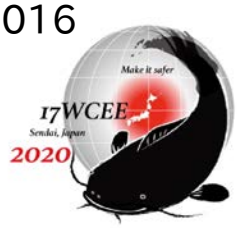

[2] Ortiz NMA. (2017). Evaluación de la vulnerabilidad sísmica post sismo 8,4 (M_w), Illapel, Chile. Aplicación al colegio San Rafael de Rozas. *Universidad Austral de Chile, Valdivia*.

[3] CSN (2020). Centro Sismológico Nacional Universidad de Chile. Available at http://www.sismologia.cl. Last access: 2020.

[4] Nakamura Y. (1989). A Method for Dynamic Characteristics Estimation of Surface Using Microtremor on the Ground Surface. *Railway Technical Research Institute*, Report 30.1.

[5] Castellaro S, Mulargia F. (2009). V_{s30} estimates using constrained H/V Measurements. *Seismological Society of America*. **99**(2A):761-773.

[6] Louie JN. (2001). Faster, better: Shear-wave velocity to 100 meters depth from refraction microtremor arrays. *Seismological Society of America*. **91**(2):347-364.

[7] Brincker R, Ventura C. (2015). *Introduction to Operational Modal Analysis*. John Wiley.

[8] Vera F. (2015). Prototipo de sistema difuso para la evaluación de la habitabilidad y accesibilidad de una edificación Post Sismo. *Universidad Austral de Chile, Valdivia*.

[9] NCh 2123. (2003). *Albañilería confinada - Requisitos de diseño y cálculo*. Instituto nacional de normalización (Chile).

[10] NCh 433. (2009). *Diseño sísmico de edificios*. Instituto nacional de normalización (Chile).

[11] Paulay T, Priestly MJN (1992). *Seismic Design of Reinforced Concrete and Masonry Buildings*. John Wiley.

[12] SESAME European Research Project (2004). Guidelines for the implementation of the H/V spectral ratio technique on ambient vibrations. Measurements, Processing and Interpretation. *European Commission - Research General Directorate*.

[13] Foti S. (2000). Multi-station Methods for Geotechnical Characterization Using Surface Waves. *Ph. D. Dissertation*, Politecnico di Torino.

[14] Decreto 61. (2011). *Reglamento que fija el diseño sísmico de edificios*. Ministerio de vivienda y urbanismo. Instituto nacional de normalización (Chile).

[15] EN-1998. (2005). *Eurocode 8: Design of structures for earthquake resistance*. European Committee for Standardization.

[16] ASCE/SEI 7-16. (2016). *Minimum design loads and Associated Criteria for buildings and other structures*. American Society of Civil Engineers.

[17] CSI (Computers & Structures Inc.) (2012). CSI Analysis Reference Manual for SAP2000®, ETABS®, and SAFE™, available from www.comp-engineering.com.

[18] PCA. (1946). *Concrete Pavement Design for Roads and Streets Carrying All Classes of Traffic*. Portland Cement Association.

[19] Bowles J.E. (1997). *Foundation Analysis and Design*. McGraw-Hill.

[20] NCh 430. (2007). *Hormigón armado. Requisitos de diseño y cálculo*. Instituto nacional de normalización (Chile).

[21] NCh 204. (2006). *Acero. Barras laminadas en caliente para hormigón armado*. Instituto nacional de normalización (Chile).

[22] NCh 1537. (2009). *Diseño estructural de edificios. Cargas Permanentes y Sobrecargas de Uso*. Instituto nacional de normalización (Chile).

[23] EN-1996. (2005). *Eurocode 6: Design of masonry structures*. European Committee for Standardization.

